PROCEEDINGS OF SCIENCE

ONLINE ICRC 2021
THE ASTROPARTICLE PHYSICS CONFERENCE
Berlin | Germany
37th International Cosmic Ray Conference
12–23 July 2021

Seasonal Variations of the Unfolded Atmospheric Neutrino Spectrum with IceCube

The IceCube Collaboration
(a complete list of authors can be found at the end of the proceedings)
E-mail: karolin.hymon@tu-dortmund.de, tim.ruhe@tu-dortmund.de

The IceCube Neutrino Observatory is a detector array at the South Pole with the central aim of studying astrophysical neutrinos. However, the majority of the detected neutrinos originates from cosmic ray interactions in the atmosphere. The rate of these atmospheric neutrinos shows a seasonal variation indicating that the rate changes with the temperature in the stratosphere. These seasonal changes of the atmospheric neutrino energy spectrum will be investigated using the Dortmund Spectrum Estimation Algorithm (DSEA). Based on results obtained from 10% of IceCube's atmospheric muon neutrino data, taken between 2011 and 2018, the differences of the measured fluxes during the Austral summer and winter will be discussed.

Corresponding authors: Karolin Hymon[1*], Tim Ruhe[1]
[1] *Department of Physics, TU Dortmund University, 44221 Dortmund, Germany*
[*] Presenter

37th International Cosmic Ray Conference (ICRC 2021)
July 12th – 23rd, 2021
Online – Berlin, Germany

PoS(ICRC2021)1159

1. Introduction

The atmospheric neutrino spectrum imposes, additionally to cosmic air shower physics, the main background in the measurement of astrophysical neutrinos. Since the observed rate of atmospheric neutrinos correlates with the atmospheric temperature [1–3], a seasonal variation of the energy spectrum is expected to occur at energies above approximately 100 GeV [4]. In this contribution, we present an analysis of the atmospheric muon neutrino spectrum using unfolding techniques to investigate the detection of seasonal variations from 8 years of IceCube data.

IceCube is a cubic-kilometer neutrino detector installed in the ice at the geographic South Pole between depths of 1450 m and 2450 m, completed in 2010. Reconstruction of the direction, energy and flavor of the neutrinos relies on the optical detection of Cherenkov radiation emitted by charged particles produced in the interactions of neutrinos in the surrounding ice or the nearby bedrock [5].

The majority of the detected neutrinos originates from meson decays in the muonic component of cosmic ray air showers. Whether these mesons decay directly into muons and neutrinos, or produce secondary mesons, depends on the local air density of the atmosphere [2]. The resulting muon neutrino (ν_μ) and anti-neutrino ($\bar{\nu}_\mu$) flux is given by the integration of the neutrino production yield over the slant depth X,

$$\Phi_\nu(E_\nu, \Theta, X) = \Phi_{\mathrm{N}}(E_\nu) \cdot \int_0^{X_{\mathrm{ground}}} \left(\frac{A_{\pi\to\nu}(X)}{1 + B_{\pi\to\nu}(X) \cdot \frac{E_\nu \cos(\Theta^\star)}{\epsilon_\pi(T(X))}} + \frac{A_{K\to\nu}(X)}{1 + B_{K\to\nu}(X) \cdot \frac{E_\nu \cos(\Theta^\star)}{\epsilon_K(T(X))}} \right) \mathrm{d}X, \quad (1)$$

with the primary cosmic ray flux $\Phi_{\mathrm{N}}(E_\nu)$ of nucleon N at neutrino energy E_ν [6]; the quantity $A_{i\to\nu}$ accounts for decay branching ratios, $B_{i\to\nu}$ for the cross sections; the denominator characterizes the competition between kaon and pion decays and the production of secondary mesons.

The latter process is favored at critical energies ϵ_i above $E_\nu \cdot \cos(\Theta^\star)$ at the zenith angle of neutrino production $\Theta^\star$. In this scenario the neutrino spectrum follows a steep power law $E^{-\gamma}$ with a spectral index of approximately $\gamma \approx 3.7$ [2]. Since the critical energy at a given atmospheric depth is anti-proportional to the air density, it is affected by temperature changes [6]. Hence, the temperature becomes linearly correlated to the critical energy assuming the atmospheric isothermal approximation of the ideal gas law. The critical energies for kaons and pions are $\epsilon_\pi \approx 125$ GeV and $\epsilon_K \approx 850$ GeV [6].

The neutrino flux at South Pole based on the NRLMSISE-00 atmospheric model [7] is displayed in Fig. 1 [4]. As expected, a distinct variation can be observed above the respective critical energies, further increasing with the neutrino energy.

2. Spectrum Unfolding

The reconstruction of the neutrino energy spectrum relies on the indirect measurement of neutrino-induced muons by the charged-current interaction inside the ice or the bedrock [8]. However, these muons are exposed to stochastic energy losses during their propagation through the detector [9] and in addition, the energy reconstruction is smeared by the limited detector resolution [8]. The neutrino energy spectrum has to be inferred from the reconstructed muon energy. This

technique is denoted as an inverse problem in unfolding, which is commonly defined by the Fredholm integral equation of the first kind [10]. In practice, an adequate algorithm is required to solve for the discrete problem set,

$$\vec{g}(y) = \mathbf{A}(E_\nu, y)\vec{f}(E_\nu), \tag{2}$$

where the spectral energy distribution $\vec{f}(E_\nu)$ of the neutrinos has to be estimated from energy-dependent detector observables y. The response matrix $\mathbf{A}(E_\nu, y)$ accounts for propagation and detection effects and displays the smearing of the energy estimation.

In this analysis, the neutrino energy spectrum is determined by the Dortmund Spectrum Estimation Algorithm (DSEA) [11–14]. The inverse problem is treated as a multinomial classification task that is solved by an arbitrary supervised machine learning classifier. The classifier's predictions are accumulated for each pre-defined energy bin and the estimate is then updated iteratively to overcome potential biases. Supplementary regularization methods within DSEA allow a scaling of the current estimate and thus accelerate the convergence behavior.

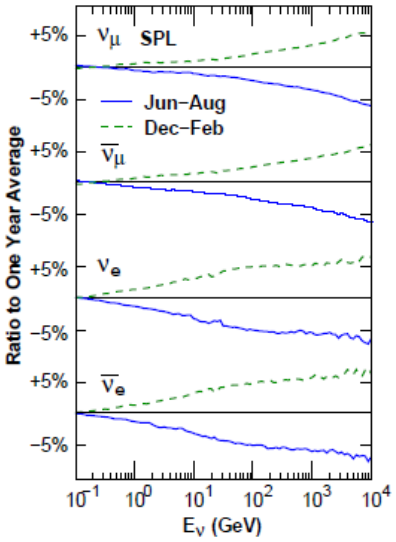

Figure 1: Ratio of the calculated neutrino flux for the Austral summer and winter at South Pole for the zenith region between 90° to 120° compared to the yearly average [4].

The internal regularization parameters, the classifier selection and its internal settings are investigated in a tenfold cross-validation approach using simulated events from the IceCube neutrino-generator (NuGen) [15]. These events are generated with the assumption of an E^{-2} power-law neutrino flux and are weighted to the atmospheric neutrino flux model Honda2006 [16] to compensate for an over-representation of high energy events in the simulation sample. The optimization procedure yields the most accurate spectrum approximation measured by the Wasserstein Distance [17] with a default random forest classifier [18] in combination with exponential step-size decay regularization in seven iterations of DSEA.

2.1 Analysis Scheme

The seasonal spectra are obtained in ten logarithmic energy bins between 125 GeV and 10 TeV. Over- and underflow bins account for events outside of the respective interval. Multiple combinations of energy-dependent quantities are investigated in terms of acceptable coverage and minimal bias in 2000 trials of DSEA. The final selection consists of the number of hit DOMs, the number of direct hits, and the truncated neutrino energy: the number of direct hits is defined assuming unscattered photons which arrive within a time residual from −15 ns to 75 ns; the truncated energy is derived from the muon energy loss [9, 19].

To account for statistical fluctuations in the unfolding, the spectral distributions are bootstrapped [20, 21]. Each data set is sampled by replacement and deconvolved with optimized DSEA. The final event spectra are determined by the average over 2000 deconvolutions, so that the standard deviation approximates the statistical uncertainty of the unfolding. Correcting for the effective detection area, livetime, and solid angle, the event spectra are transformed into a differential neutrino flux [8].

2.2 Event Selection

To study the seasonal effects on the atmospheric neutrino flux, the diffuse upgoing event sample which contains upward moving muons, as described in Ref. [22], is divided into separate seasons. The analysis is developed using 10% of the data taken between January 2011 and December 2018. Only events from the Southern Hemisphere in the zenith range from 90° to 120° are selected, excluding tropical latitudes between 120° to 135°. This results in a total of 35 038 events within 278 days of livetime, corresponding to approx. 3000 events per month.

2.3 Systematic Uncertainties

Since DSEA is trained on simulated events, the unfolded energy spectra are affected by systematic uncertainties in the detector simulation. The impact of these effects is estimated from simulations with varied parameters, similar to the approaches presented in [8, 23]. These generated events are treated as pseudo-data and are sampled according to the atmospheric neutrino flux model Honda2006 [16]. The ratio of the unfolded spectrum to the reference unfolding with the default systematic parameters is the systematic uncertainty of the parameter variation. Each uncertainty is combined in the squared sum for positive and negative deviations to the reference result and the total systematic uncertainty is given by,

$$\sigma_{\text{sys}} = \sqrt{\sigma^2_{\text{DOM}} + \sigma^2_{\text{abs}} + \sigma^2_{\text{scat}} + \sigma^2_{\text{flux}}}, \tag{3}$$

with the uncertainty caused by the efficiency of the optical modules σ_{DOM}, the absorption and scattering coefficients of the ice model σ_{abs} and σ_{scat}, and the atmospheric neutrino flux model σ_{flux}.

Monte Carlo simulations from the same NuGen sample are used for the first three systematic parameters. The DOM efficiency was scaled by ±10% [5]. Propagation effects of photons in the ice are described by absorption and scattering coefficients. The simulated events are obtained from the *SpiceLea* ice model, which accounts for the depth-dependence of both coefficients [24] and anisotropies in the xy-plane of the detection volume [25]. The dependence of both coefficients on one another are taken into account by a joint reduction of −7% as a lower bound for absorption and scattering. The upper bound is then determined for each parameter individually, increasing each by +10%. The uncertainties induced by the ice model coefficients can be combined by Eq. (3) into a total uncertainty of photon propagation effects.

Since the simulated events are weighted to a flux model for the algorithm optimization and determination of the systematic uncertainties, the flux model imposes an additional uncertainty on the unfolded spectra. To estimate the impact of flux model uncertainties on the unfolded spectrum, the reference simulation is weighted according to the lower and upper flux limits. As illustrated in Ref. [16], the flux uncertainty scales linearly from 100 GeV to 1 TeV assuming an uncertainty of

14% at 100 GeV and 25% at 1 TeV. The uncertainty remains approximately constant at energies between 1 TeV to 10 TeV.

To obtain an absolute measurement of seasonal neutrino fluxes, other sources of systematic uncertainties, such as assumptions about the primary cosmic ray spectrum, would have to be considered. However, since the central aim is to determine the seasonal variations with respect to the annual mean of the neutrino flux, the model independence of deconvolution is exploited and the variations are measured relatively to the annual mean. Assuming that the investigated detector systematics remain constant throughout the year, merely the propagation of statistical uncertainties impacts the flux deviation to the yearly average.

3. Results

The unfolded energy spectra for Austral summer and winter are displayed in Fig. 2(a). Both spectra agree within the uncertainties. Comparing the seasonal fluxes to the annual mean, a tendency towards an increased flux for the period from December to February is observable. The flux for the period from June to August remains smaller accordingly. A deviation around 1 TeV might be due to artifacts in the training sample. This was investigated in deconvolutions of monthly data sets.

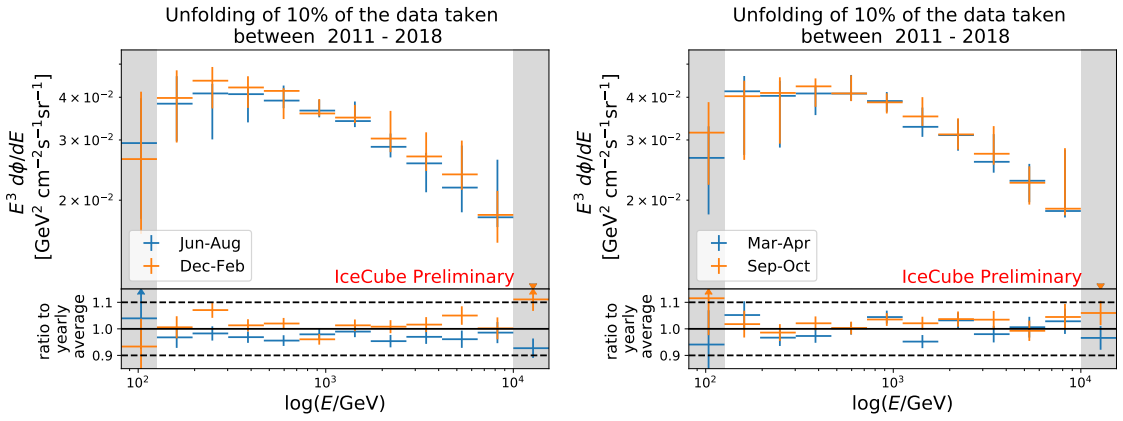

(a) Austral summer and winter

(b) Austral spring and autumn

Figure 2: Unfolded seasonal muon neutrino spectra with statistical and systematic uncertainties using 10% of the muon neutrino data from IceCube between 2011 and 2018 for the zenith range between 90° to 120°. The ratio to the unfolded flux averaged over all seasons is displayed below neglecting systematic uncertainties. First tendencies towards an increased flux in the Austral summer from December to February is observable despite large statistical uncertainties. The spectra for autumn and spring, on the other hand, are in agreement with the annual mean.

The unfolded spectra for the Austral spring and autumn are displayed in Fig. 2(b) as a test of the unfolding method. Since both seasons should have similar temperature profiles, both spectra are expected to be in agreement. The data sets are constructed from events within two months from March to April and September to October to provide a clear demarcation between seasons. The seasonal energy spectra agree within the uncertainties and with the annual mean unfolded neutrino flux.

After the discussion of the unfolded spectra obtained from 10% of the data taken from 2011 to 2018, the detection potential of seasonal variations using the complete data set is investigated on Monte Carlo simulations. For this, the simulated neutrino events are sampled according to the seasonal flux model presented in Ref. [4]. The number of events and the livetime of both pseudo-data sets were increased by a factor of ten. The deconvolved spectra are denoted in Fig. 3 with the associated uncertainties. Compared to the tests on 10% of the data taken between 2011 and 2018, the uncertainties decrease significantly and the relationship of the seasonal neutrino fluxes to each other can be clearly observed below. This estimation yields a deviation of approx. 2% to 8% between the Austral summer and winter.

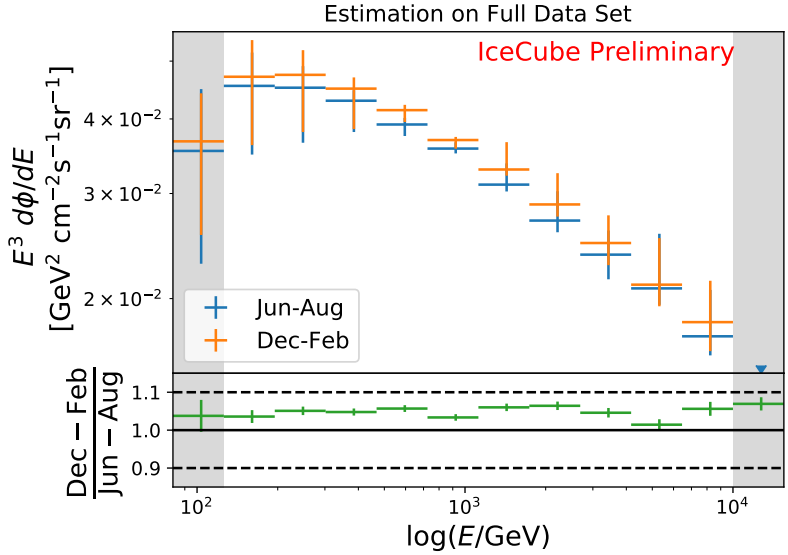

Figure 3: Estimation of the unfolded seasonal spectra for the Austral summer and winter using all events from 2011 to 2018 as pseudo-data. Two sets are constructed by the Monte Carlo simulation weighted to the seasonal prediction from Ref. [4]; scaling the number of events and livetime by a factor of ten. Both sets are then unfolded with DSEA and scaled to a differential flux. The ratio between the seasonal unfolded fluxes is displayed below in terms of statistical uncertainties.

4. Conclusion and Outlook

The presented analysis holds a great potential for detecting seasonal variations of the atmospheric neutrino energy spectrum with IceCube data. Initial tendencies towards an increased flux in the Austral summer are evident on 10% of the present atmospheric muon neutrino data set including events from 2011 to 2018. Due to the relative comparison of seasonal energy spectra, the analysis becomes independent of systematic uncertainties in the detector simulation and other model assumptions. An extension by a factor of ten to the entire data set would decrease the statistical uncertainty by the square root of ten, making seasonal variations to the unfolded annual mean flux more apparent. The sample can be extended to 9 years of data, further decreasing the statistical uncertainty, in particular at higher energies in the TeV-regime.

Further improvements of this analysis are in progress. The significance of the of the measured variations will be determined on 10% of the recorded data. The hypothesis of observing no seasonal variations with respect to the annual mean will be investigated for each energy bin and season. Using the full 9-year data sample will potentially allow measurements of the monthly neutrino spectra with sufficient statistics for the first time.

References

[1] **IceCube** Collaboration *PoS* **ICRC2011** (2012) 662.

[2] **IceCube** Collaboration *PoS* **ICRC2013** (2014) 0492.

[3] **IceCube** Collaboration *PoS* **ICRC2019** (2020) 465.

[4] M. Honda, M. Sajjad Athar, T. Kajita, K. Kasahara, and S. Midorikawa *Phys. Rev. D* **92** (2015) 023004.

[5] **IceCube** Collaboration, M. G. Aartsen *et al. JINST* **12** no. 03, (2017) P03012.

[6] T. K. Gaisser, *Cosmic rays and particle physics*. Cambridge University Press, 1990.

[7] J. Picone, A. Hedin, D. Drob, and A. Aikin *Journal of Geophysical Research* **107** (12, 2002) .

[8] **IceCube** Collaboration, M. G. Aartsen *et al. Eur. Phys. J. C* **75** no. 3, (2015) 116.

[9] **IceCube** Collaboration, R. Abbasi *et al. Nucl. Instrum. Meth. A* **703** (2013) 190–198.

[10] I. Fredholm *Acta Math.* **27** (1903) 365.

[11] M. Bunse *https://sfb876.tu-dortmund.de/deconvolution/index.html* .

[12] T. Ruhe, M. Schmitz, T. Voigt, and M. Wornowizki *PoS* **ICRC2013** (2014) 3354.

[13] T. Ruhe, T. Voigt, M. Wornowizki, M. Börner, W. Rhode, and K. Morik *Astronomical Data Analysis Software and Systems XXVI* **521** (2019) .

[14] L. Kardum *PoS* **ICRC2021** (these proceedings) xyz.

[15] A. Gazizov and M. P. Kowalski *Comput. Phys. Commun.* **172** (2005) 203.

[16] M. Honda, T. Kajita, K. Kasahara, S. Midorikawa, and T. Sanuki *Phys. Rev. D* **75** (2007) 043006.

[17] A. Ramdas, N. Garcia, and M. Cuturi *Entropy* **19** (2015) .

[18] F. Pedregosa, G. Varoquaux, A. Gramfort, V. Michel, B. Thirion, O. Grisel, M. Blondel, P. Prettenhofer, R. Weiss, V. Dubourg, J. Vanderplas, A. Passos, D. Cournapeau, M. Brucher, M. Perrot, and E. Duchesnay *Journal of Machine Learning Research* **12** (2011) 2825–2830.

[19] **AMANDA** Collaboration, J. Ahrens *et al. Phys. Rev. D* **66** (2002) 012005.

[20] T. Hastie, J. Friedman, and R. Tibshirani, *The Elements of Statistical Learning: Data Mining, Inference, and Prediction*. Springer Publishing Company, Incorporated, 2017.

[21] **IceCube** Collaboration, M. G. Aartsen *et al.* *Eur. Phys. J. C* **77** no. 10, (2017) 692.

[22] **IceCube** Collaboration, M. G. Aartsen *et al.* *ApJ* **833** (2016) 3.

[23] **ANTARES** Collaboration, A. Albert *et al.* *Phys. Lett. B* **816** (2021) 136228.

[24] **IceCube** Collaboration, M. Aartsen *et al.* *Nucl. Instrum. Meth. A* **711** (2013) 73–89.

[25] **IceCube** Collaboration *PoS* **ICRC2013** (2014) 0580.

Full Author List: IceCube Collaboration

R. Abbasi[17], M. Ackermann[59], J. Adams[18], J. A. Aguilar[12], M. Ahlers[22], M. Ahrens[50], C. Alispach[28], A. A. Alves Jr.[31], N. M. Amin[42], R. An[14], K. Andeen[40], T. Anderson[56], G. Anton[26], C. Argüelles[14], Y. Ashida[38], S. Axani[15], X. Bai[46], A. Balagopal V.[38], A. Barbano[28], S. W. Barwick[30], B. Bastian[59], V. Basu[38], S. Baur[12], R. Bay[8], J. J. Beatty[20, 21], K.-H. Becker[58], J. Becker Tjus[11], C. Bellenghi[27], S. BenZvi[48], D. Berley[19], E. Bernardini[59, 60], D. Z. Besson[34, 61], G. Binder[8, 9], D. Bindig[58], E. Blaufuss[19], S. Blot[59], M. Boddenberg[1], F. Bontempo[31], J. Borowka[1], S. Böser[39], O. Botner[57], J. Böttcher[1], E. Bourbeau[22], F. Bradascio[59], J. Braun[38], S. Bron[28], J. Brostean-Kaiser[59], S. Browne[32], A. Burgman[57], R. T. Burley[2], R. S. Busse[41], M. A. Campana[45], E. G. Carnie-Bronca[2], C. Chen[6], D. Chirkin[38], K. Choi[52], B. A. Clark[24], K. Clark[33], L. Classen[41], A. Coleman[42], G. H. Collin[15], J. M. Conrad[15], P. Coppin[13], P. Correa[13], D. F. Cowen[55, 56], R. Cross[48], C. Dappen[1], P. Dave[6], C. De Clercq[13], J. J. DeLaunay[56], H. Dembinski[42], K. Deoskar[50], S. De Ridder[29], A. Desai[38], P. Desiati[38], K. D. de Vries[13], G. de Wasseige[13], M. de With[10], T. DeYoung[24], S. Dharani[1], A. Diaz[15], J. C. Díaz-Vélez[38], M. Dittmer[41], H. Dujmovic[31], M. Dunkman[56], M. A. DuVernois[38], E. Dvorak[46], T. Ehrhardt[39], P. Eller[27], R. Engel[31, 32], H. Erpenbeck[1], J. Evans[19], P. A. Evenson[42], K. L. Fan[19], A. R. Fazely[7], S. Fiedlschuster[26], A. T. Fienberg[56], K. Filimonov[8], C. Finley[50], L. Fischer[59], D. Fox[55], A. Franckowiak[11, 59], E. Friedman[19], A. Fritz[39], P. Fürst[1], T. K. Gaisser[42], J. Gallagher[37], E. Ganster[1], A. Garcia[14], S. Garrappa[59], L. Gerhardt[9], A. Ghadimi[54], C. Glaser[57], T. Glauch[27], T. Glüsenkamp[26], A. Goldschmidt[9], J. G. Gonzalez[42], S. Goswami[54], D. Grant[24], T. Grégoire[56], S. Griswold[48], M. Gündüz[11], C. Günther[1], C. Haack[27], A. Hallgren[57], R. Halliday[24], L. Halve[1], F. Halzen[38], M. Ha Minh[27], K. Hanson[38], J. Hardin[38], A. A. Harnisch[24], A. Haungs[31], S. Hauser[1], D. Hebecker[10], K. Helbing[58], F. Henningsen[27], E. C. Hettinger[24], S. Hickford[58], J. Hignight[25], C. Hill[16], G. C. Hill[2], K. D. Hoffman[19], R. Hoffmann[58], T. Hoinka[23], B. Hokanson-Fasig[38], K. Hoshina[38, 62], F. Huang[56], M. Huber[27], T. Huber[31], K. Hultqvist[50], M. Hünnefeld[23], R. Hussain[38], S. In[52], N. Iovine[12], A. Ishihara[16], M. Jansson[50], G. S. Japaridze[5], M. Jeong[52], B. J. P. Jones[4], D. Kang[31], W. Kang[52], X. Kang[45], A. Kappes[41], D. Kappesser[39], T. Karg[59], M. Karl[27], A. Karle[38], U. Katz[26], M. Kauer[38], M. Kellermann[1], J. L. Kelley[38], A. Kheirandish[56], K. Kin[16], T. Kintscher[59], J. Kiryluk[51], S. R. Klein[8, 9], R. Koirala[42], H. Kolanoski[10], T. Kontrimas[27], L. Köpke[39], C. Kopper[24], S. Kopper[54], D. J. Koskinen[22], P. Koundal[31], M. Kovacevich[45], M. Kowalski[10, 59], T. Kozynets[22], E. Kun[11], N. Kurahashi[45], N. Lad[59], C. Lagunas Gualda[59], J. L. Lanfranchi[56], M. J. Larson[19], F. Lauber[58], J. P. Lazar[14, 38], J. W. Lee[52], K. Leonard[38], A. Leszczyńska[32], Y. Li[56], M. Lincetto[11], Q. R. Liu[38], M. Liubarska[25], E. Lohfink[39], C. J. Lozano Mariscal[41], L. Lu[38], F. Lucarelli[28], A. Ludwig[24, 35], W. Luszczak[38], Y. Lyu[8, 9], W. Y. Ma[59], J. Madsen[38], K. B. M. Mahn[24], Y. Makino[38], S. Mancina[38], I. C. Mariş[12], R. Maruyama[43], K. Mase[16], T. McElroy[25], F. McNally[36], J. V. Mead[22], K. Meagher[38], A. Medina[21], M. Meier[16], S. Meighen-Berger[27], J. Micallef[24], D. Mockler[12], T. Montaruli[28], R. W. Moore[25], R. Morse[38], M. Moulai[15], R. Naab[59], R. Nagai[16], U. Naumann[58], J. Necker[59], L. V. Nguyễn[24], H. Niederhausen[27], M. U. Nisa[24], S. C. Nowicki[24], D. R. Nygren[9], A. Obertacke Pollmann[58], M. Oehler[31], A. Olivas[19], E. O'Sullivan[57], H. Pandya[42], D. V. Pankova[56], N. Park[33], G. K. Parker[4], E. N. Paudel[42], L. Paul[40], C. Pérez de los Heros[57], L. Peters[1], J. Peterson[38], S. Philippen[1], D. Pieloth[23], S. Pieper[58], M. Pittermann[32], A. Pizzuto[38], M. Plum[40], Y. Popovych[39], A. Porcelli[29], M. Prado Rodriguez[38], P. B. Price[8], B. Pries[24], G. T. Przybylski[9], C. Raab[12], A. Raissi[18], M. Rameez[22], K. Rawlins[3], I. C. Rea[27], A. Rehman[42], P. Reichherzer[11], R. Reimann[1], G. Renzi[12], E. Resconi[27], S. Reusch[59], W. Rhode[23], M. Richman[45], B. Riedel[38], E. J. Roberts[2], S. Robertson[8, 9], G. Roellinghoff[52], M. Rongen[39], C. Rott[49, 52], T. Ruhe[23], D. Ryckbosch[29], D. Rysewyk Cantu[24], I. Safa[14, 38], J. Saffer[32], S. E. Sanchez Herrera[24], A. Sandrock[23], J. Sandroos[39], M. Santander[54], S. Sarkar[44], S. Sarkar[25], K. Satalecka[59], M. Scharf[1], M. Schaufel[1], H. Schieler[31], S. Schindler[26], P. Schlunder[23], T. Schmidt[19], A. Schneider[38], J. Schneider[26], F. G. Schröder[31, 42], L. Schumacher[27], G. Schwefer[1], S. Sclafani[45], D. Seckel[42], S. Seunarine[47], A. Sharma[57], S. Shefali[32], M. Silva[38], B. Skrzypek[14], B. Smithers[4], R. Snihur[38], J. Soedingrekso[23], D. Soldin[42], C. Spannfellner[27], G. M. Spiczak[47], C. Spiering[59, 61], J. Stachurska[59], M. Stamatikos[21], T. Stanev[42], R. Stein[59], J. Stettner[1], A. Steuer[39], T. Stezelberger[9], T. Stürwald[58], T. Stuttard[22], G. W. Sullivan[19], I. Taboada[6], F. Tenholt[11], S. Ter-Antonyan[7], S. Tilav[42], F. Tischbein[1], K. Tollefson[24], L. Tomankova[11], C. Tönnis[53], S. Toscano[12], D. Tosi[38], A. Trettin[59], M. Tselengidou[26], C. F. Tung[6], A. Turcati[27], R. Turcotte[31], C. F. Turley[56], J. P. Twagirayezu[24], B. Ty[38], M. A. Unland Elorrieta[41], N. Valtonen-Mattila[57], J. Vandenbroucke[38], N. van Eijndhoven[13], D. Vannerom[15], J. van Santen[59], S. Verpoest[29], M. Vraeghe[29], C. Walck[50], T. B. Watson[4], C. Weaver[24], P. Weigel[15], A. Weindl[31], M. J. Weiss[56], J. Weldert[39], C. Wendt[38], J. Werthebach[23], M. Weyrauch[32], N. Whitehorn[24, 35], C. H. Wiebusch[1], D. R. Williams[54], M. Wolf[27], K. Woschnagg[8], G. Wrede[26], J. Wulff[11], X. W. Xu[7], Y. Xu[51], J. P. Yanez[25], S. Yoshida[16], S. Yu[24], T. Yuan[38], Z. Zhang[51]

[1] III. Physikalisches Institut, RWTH Aachen University, D-52056 Aachen, Germany
[2] Department of Physics, University of Adelaide, Adelaide, 5005, Australia
[3] Dept. of Physics and Astronomy, University of Alaska Anchorage, 3211 Providence Dr., Anchorage, AK 99508, USA
[4] Dept. of Physics, University of Texas at Arlington, 502 Yates St., Science Hall Rm 108, Box 19059, Arlington, TX 76019, USA
[5] CTSPS, Clark-Atlanta University, Atlanta, GA 30314, USA
[6] School of Physics and Center for Relativistic Astrophysics, Georgia Institute of Technology, Atlanta, GA 30332, USA
[7] Dept. of Physics, Southern University, Baton Rouge, LA 70813, USA
[8] Dept. of Physics, University of California, Berkeley, CA 94720, USA
[9] Lawrence Berkeley National Laboratory, Berkeley, CA 94720, USA
[10] Institut für Physik, Humboldt-Universität zu Berlin, D-12489 Berlin, Germany
[11] Fakultät für Physik & Astronomie, Ruhr-Universität Bochum, D-44780 Bochum, Germany
[12] Université Libre de Bruxelles, Science Faculty CP230, B-1050 Brussels, Belgium
[13] Vrije Universiteit Brussel (VUB), Dienst ELEM, B-1050 Brussels, Belgium
[14] Department of Physics and Laboratory for Particle Physics and Cosmology, Harvard University, Cambridge, MA 02138, USA
[15] Dept. of Physics, Massachusetts Institute of Technology, Cambridge, MA 02139, USA

[16] Dept. of Physics and Institute for Global Prominent Research, Chiba University, Chiba 263-8522, Japan
[17] Department of Physics, Loyola University Chicago, Chicago, IL 60660, USA
[18] Dept. of Physics and Astronomy, University of Canterbury, Private Bag 4800, Christchurch, New Zealand
[19] Dept. of Physics, University of Maryland, College Park, MD 20742, USA
[20] Dept. of Astronomy, Ohio State University, Columbus, OH 43210, USA
[21] Dept. of Physics and Center for Cosmology and Astro-Particle Physics, Ohio State University, Columbus, OH 43210, USA
[22] Niels Bohr Institute, University of Copenhagen, DK-2100 Copenhagen, Denmark
[23] Dept. of Physics, TU Dortmund University, D-44221 Dortmund, Germany
[24] Dept. of Physics and Astronomy, Michigan State University, East Lansing, MI 48824, USA
[25] Dept. of Physics, University of Alberta, Edmonton, Alberta, Canada T6G 2E1
[26] Erlangen Centre for Astroparticle Physics, Friedrich-Alexander-Universität Erlangen-Nürnberg, D-91058 Erlangen, Germany
[27] Physik-department, Technische Universität München, D-85748 Garching, Germany
[28] Département de physique nucléaire et corpusculaire, Université de Genève, CH-1211 Genève, Switzerland
[29] Dept. of Physics and Astronomy, University of Gent, B-9000 Gent, Belgium
[30] Dept. of Physics and Astronomy, University of California, Irvine, CA 92697, USA
[31] Karlsruhe Institute of Technology, Institute for Astroparticle Physics, D-76021 Karlsruhe, Germany
[32] Karlsruhe Institute of Technology, Institute of Experimental Particle Physics, D-76021 Karlsruhe, Germany
[33] Dept. of Physics, Engineering Physics, and Astronomy, Queen's University, Kingston, ON K7L 3N6, Canada
[34] Dept. of Physics and Astronomy, University of Kansas, Lawrence, KS 66045, USA
[35] Department of Physics and Astronomy, UCLA, Los Angeles, CA 90095, USA
[36] Department of Physics, Mercer University, Macon, GA 31207-0001, USA
[37] Dept. of Astronomy, University of Wisconsin–Madison, Madison, WI 53706, USA
[38] Dept. of Physics and Wisconsin IceCube Particle Astrophysics Center, University of Wisconsin–Madison, Madison, WI 53706, USA
[39] Institute of Physics, University of Mainz, Staudinger Weg 7, D-55099 Mainz, Germany
[40] Department of Physics, Marquette University, Milwaukee, WI, 53201, USA
[41] Institut für Kernphysik, Westfälische Wilhelms-Universität Münster, D-48149 Münster, Germany
[42] Bartol Research Institute and Dept. of Physics and Astronomy, University of Delaware, Newark, DE 19716, USA
[43] Dept. of Physics, Yale University, New Haven, CT 06520, USA
[44] Dept. of Physics, University of Oxford, Parks Road, Oxford OX1 3PU, UK
[45] Dept. of Physics, Drexel University, 3141 Chestnut Street, Philadelphia, PA 19104, USA
[46] Physics Department, South Dakota School of Mines and Technology, Rapid City, SD 57701, USA
[47] Dept. of Physics, University of Wisconsin, River Falls, WI 54022, USA
[48] Dept. of Physics and Astronomy, University of Rochester, Rochester, NY 14627, USA
[49] Department of Physics and Astronomy, University of Utah, Salt Lake City, UT 84112, USA
[50] Oskar Klein Centre and Dept. of Physics, Stockholm University, SE-10691 Stockholm, Sweden
[51] Dept. of Physics and Astronomy, Stony Brook University, Stony Brook, NY 11794-3800, USA
[52] Dept. of Physics, Sungkyunkwan University, Suwon 16419, Korea
[53] Institute of Basic Science, Sungkyunkwan University, Suwon 16419, Korea
[54] Dept. of Physics and Astronomy, University of Alabama, Tuscaloosa, AL 35487, USA
[55] Dept. of Astronomy and Astrophysics, Pennsylvania State University, University Park, PA 16802, USA
[56] Dept. of Physics, Pennsylvania State University, University Park, PA 16802, USA
[57] Dept. of Physics and Astronomy, Uppsala University, Box 516, S-75120 Uppsala, Sweden
[58] Dept. of Physics, University of Wuppertal, D-42119 Wuppertal, Germany
[59] DESY, D-15738 Zeuthen, Germany
[60] Università di Padova, I-35131 Padova, Italy
[61] National Research Nuclear University, Moscow Engineering Physics Institute (MEPhI), Moscow 115409, Russia
[62] Earthquake Research Institute, University of Tokyo, Bunkyo, Tokyo 113-0032, Japan

Acknowledgements

USA – U.S. National Science Foundation-Office of Polar Programs, U.S. National Science Foundation-Physics Division, U.S. National Science Foundation-EPSCoR, Wisconsin Alumni Research Foundation, Center for High Throughput Computing (CHTC) at the University of Wisconsin–Madison, Open Science Grid (OSG), Extreme Science and Engineering Discovery Environment (XSEDE), Frontera computing project at the Texas Advanced Computing Center, U.S. Department of Energy-National Energy Research Scientific Computing Center, Particle astrophysics research computing center at the University of Maryland, Institute for Cyber-Enabled Research at Michigan State University, and Astroparticle physics computational facility at Marquette University; Belgium – Funds for Scientific Research (FRS-FNRS and FWO), FWO Odysseus and Big Science programmes, and Belgian Federal Science Policy Office (Belspo); Germany – Bundesministerium für Bildung und Forschung (BMBF), Deutsche Forschungsgemeinschaft (DFG), Helmholtz Alliance for Astroparticle Physics (HAP), Initiative and Networking Fund of the Helmholtz Association, Deutsches Elektronen Synchrotron (DESY), and High Performance Computing cluster of the RWTH Aachen; Sweden – Swedish Research Council, Swedish Polar Research Secretariat, Swedish National Infrastructure for Computing (SNIC), and Knut and Alice Wallenberg Foundation; Australia – Australian

Research Council; Canada – Natural Sciences and Engineering Research Council of Canada, Calcul Québec, Compute Ontario, Canada Foundation for Innovation, WestGrid, and Compute Canada; Denmark – Villum Fonden and Carlsberg Foundation; New Zealand – Marsden Fund; Japan – Japan Society for Promotion of Science (JSPS) and Institute for Global Prominent Research (IGPR) of Chiba University; Korea – National Research Foundation of Korea (NRF); Switzerland – Swiss National Science Foundation (SNSF); United Kingdom – Department of Physics, University of Oxford.